Semiconductor Physics, Quantum Electronics & Optoelectronics, 2009. V. 12, N 1. P. 12-16.

PACS 63.41.Bn, 41.20.Nr, 71.23.-k

Computer analysis of a-SiC:H/c-Si heterojunction solar cells

V.I. Ivashchenko
I.M. Frantsevych Institute of Problems of Material Science, NAS of Ukraine,
3, Krzhyzhanovsky str., 03142 Kyiv, Ukraine, e-mail: ivash@ipms.kiev.ua

Abstract. A computer model to simulate hybrid solar cells based on hydrogenated amorphous silicon carbide (a-SiC:H) and crystalline silicon (c-Si) was developed. Using the developed approach, the current-voltage characteristics of *p*(*n*) a-SiC:H/*n*(*p*) c-Si heterojunction solar cells were analyzed. It was shown that the maximum cell efficiency of the *p-n* and *n-p* tandems is observed for the amorphous layer thickness ~ 0.03-0.06 μm and 0.01-0.03 μm, respectively. The efficiency of the *n-p* heterojunctions is found to be higher than that of the *p-n* tandem by approximately 1.5 %. This is attributed to the fact that, in *n*-doped a-SiC:H, the conductive band tail is narrower compared to the valence band one in *p*-doped films. The simulated results are compared with the available experimental data obtained with a-SiC:H/c-Si heterostructures.

Keywords: amorphous silicon carbide, hybrid heterojunction solar cells, computer analysis, current-voltage characteristics.

Manuscript received 29.10.08; accepted for publication 18.12.08; published online 30.01.09.

1. Introduction

Recent advances in producing the solar cells based on amorphous silicon carbide have indicated the great potential for this material [1]. Amorphous hydrogenated silicon carbide (a-SiC:H) films are widely used as active layers in both amorphous-amorphous and amorphous-crystalline (polycrystalline) silicon solar cells [1-4]. a-SiC:H/c-Si heterojunctions are easy to manufacture by deposition of a thin a-SiC:H layer on top of c-Si wafers. For this purpose, plasma enhanced chemical vapor deposition (PECVD) is often used. The heterojunction solar cells have the efficiency comparable with that of crystalline cells, but, produced on the basis of low cost materials by using the energy saving technology, are cheaper than crystalline cells [3].

Up to now, *p* a-SiC:H/*n* c-Si heterojunction solar cells have been comprehensively studied by using both experimental and theoretical procedures [2-4]. In particular, the collection of photogenerated carries and the effects of temperature, illumination, doping level, band discontinuities and tunneling on the current-voltage (*I-V*) characteristics have been analyzed in detail. However, the dependence of these characteristics on the amorphous layer thickness (d_{SiC}) is not investigated. To our knowledge, *n* a-SiC:H/*p* c-Si heterojunction solar cells are not still studied by using theoretical procedures.

Therefore, we intend to fill these gaps in studying the hybrid *n-p* and *p-n* heterojunctions. In this work, both these types of heterojunction devices were investigated. For this purpose, a computational scheme was developed. We studied the parameters of the *I-V* characteristics: the short circuit current (J_{SC}), open circuit voltage (V_{OC}), filling factor (FF) and efficiency (η) as functions of the amorphous layer thickness. The influence of the valence and conduction band tail widths (T_V, T_C) on V_{OC} was analyzed. Besides, the developed scheme was employed to interpret the peculiarities of dark *I-V* characteristics.

2. Theoretical background and input data

Modeling of various photovoltaic devices is based on the simultaneous solution of the continuity and current density equations for electron, *n*, and holes, *p*, as well as the Poisson equation. Before, the models of the density of states (DOS) for a-SiC:H and c-Si should be properly constructed. We considered the valence and conduction DOSs as semi-elliptic bands over all the energetic range. The DOSs are normalized by $3N_a$ (in states/eV/cm^3 with N_a is a number of atoms per cm^3), implying that the DOS is formed from 2*p*-states only. The semi-elliptic valence and conduction DOSs are smoothly transformed to the valence and conduction band tails, N_V and N_C, respectively. The $N_V(E)$ and $N_C(E)$ distributions are approximated by the exponential-decay and -growth functions, respectively. The slope of the tails is described by characteristic energies, T_V and T_C.

In Fig. 1, we show the total model DOS of a-SiC:H. One can see that, the total DOS additionally includes the donor, N_D, (acceptor, N_A) and two dangling bond states, N_T, that are approximated by the Gaussian distribution with the energy position ($E_{\text{donor(accept)}}$ and E_{db}), density ($N_{\text{donor(accept)}}$ and N_{db}) and variance ($\sigma_{\text{donor(accept)}}$ and σ_{db}) for the donor (acceptor) and dangling bond states, respectively. The two dangling bond state distributions have the values of E_{db} equaled to 1/3 and 2/3 of the mobility band gap (E_μ), provided the zero of energy is the conduction mobility edge. The accepted model band structure of a-SiC:H was constructed taking into account the realistic DOS of amorphous silicon carbide [5].

The DOS of c-Si is similar to that of a-SiC:H, except that the energy positions, E_{db}, coincide and are equal to ½ of E_μ . The input parameters used in the model calculations are summarized in Table.

Numerical solution of the Poisson and current density equations were similar to those described by Cech for an n^+-i-n^+ device [6]. However, since we consider p-n and n-p structures, the corresponding equations should be solved for electrons and holes. Shortly, the computational scheme is as follows:

1) The space charge density, Q, as a function of the Fermi energy, E_F, is calculated from the model DOS of the $p(n)$ a-SiC:H / $n(p)$ c-Si heterostructures.

2) Using the calculated dependence $Q(E_F)$, one can find the dependence of the electrostatic potential on distance, $\psi(x)$, from the Poisson equation, following the procedure [6].

3) Further, n and p are calculated by using the procedure [6].

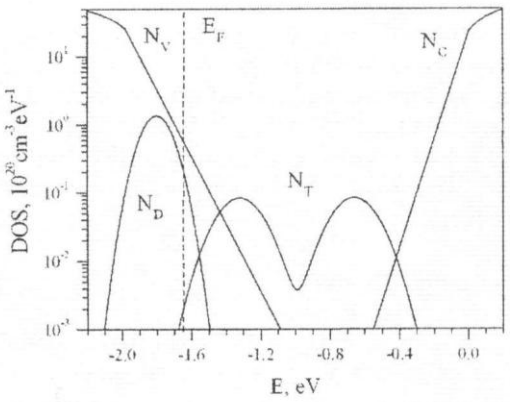

Fig. 1. Model density of states (DOS) of p-type a-SiC:H. N_V and N_C are the valence and conduction band tails, respectively; N_D is doping (donor) states; N_T is dangling bond states.

4) Accepting the Shockley-Read type of recombination and knowing the generation term and the dependences $\psi(x)$, the electron and holes currents can be found [7].

5) New distributions $n(x)$ and $p(x)$ are calculated. Since, we use the Shockley-Read recombination, n and p are found by using a self-consistent procedure.

6) New dependence $\psi(x)$ is calculated.

The items 3-6 are repeated until the convergence in the electron and hole currents is reached.

We considered the ideal ohmic contacts for both types of these heterojunctions. The photogeneration term was taken in the form suggested by Sichanugrist, Konagi and Takahashi [8].

In contrast to the traditional models [9, 10], the

Table. Parameters used for computer simulations of the $p(n)$ a-SiC:H/$n(p)$ c-Si devices. The temperature of all the devices is 300 K. The parameters for p a-SiC:H and n c-Si were similar to those used in Refs 2, 3.

Parameters	Units	p a-SiC:H/n c-Si		n a-SiC:H/p c-Si	
		p a-SiC:H	n c-Si	n a-SiC:H	p c-Si
Length of the layer, L	μm	0.005-0.150	250	0.005-0.150	250
Electron affinity, χ	eV	3.62	4.05	3.62	4.05
Mobility gap, E_μ	eV	1.98	1.12	1.98	1.12
Dielectric constants, ε		10	11.7	10	11.7
Valence band width, W_V	eV	17	16	17	16
Conduction band width, W_C	eV	16	16	16	16
Valence band tail, T_V	eV	0.088	0.00	0.88	0.00
Conduction band tail, T_C	eV	0.055	0.00	0.55	0.00
Doping level	cm^{-3}	9×10^{18}	1×10^{16}	9×10^{18}	1×10^{16}
Energy position, $E_{\text{donor(accept)}}$	eV	–1.80	–0.02	–0.18	–1.10
Variance, $\sigma_{\text{donor(accept)}}$	eV	0.08	0.02	0.08	0.02
Dangling bond density	cm^3	5×10^{18}	1×10^{12}	5×10^{18}	1×10^{12}
Variance, σ_{db}	eV	0.12	0.05	0.12	0.05
Electron mobility, μ_e	$cm^2V^{-1}s^{-1}$	4	1500	4	1500
Hole mobility, μ_h	$cm^2V^{-1}s^{-1}$	1	450	1	450
Electron recomb. time, τ_e	s^{-1}	10^{-8}	10^{-7}	10^{-8}	10^{-7}
Hole recomb. time, τ_h	s^{-1}	10^{-8}	10^{-7}	10^{-8}	10^{-7}
Absorption coefficient, $(\alpha E)^{1/2} = B(E-E_\mu)$, B	$cm^{-1/2}eV^{-1}$	240	(*)	240	(*)

(*) The absorption coefficient is in the form, suggested in Ref. 10.

developed computational scheme does not involve the descretization of the basic equations. The AM1.5 solar spectrum (100 mW/cm^2) was taken from Ref. 10. The test of the scheme was carried out by using the data calculated with the software SimWindows [10] for *p* c-Si/*n* c-Si and *p* c-SiC/*n* c-Si solar cells. Both these schemes were found to provide almost identical results (nor shown here).

3. Results and discussion

In Fig. 2, the simulated *I-V* characteristics for *p* a-SiC:H/*n* c-Si and *n* a-SiC:H/*p* c-Si heterojunction solar cells are presented. For the sake of comparison, the experimental dependence for the first tandem is also shown. We see that the calculated and experimental characteristics agree well, which validates our approach. One can see also that the *I-V* curves are sensitive to the thickness d_{SiC} in both heterostructures.

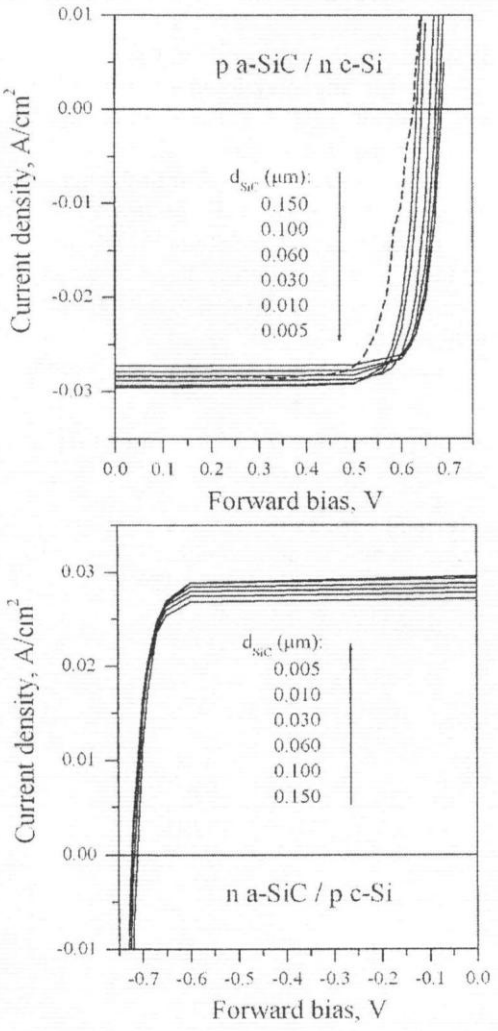

Fig. 2. Simulated *I-V* characteristics at the AM1.5 100 mW/cm^2 illumination of the *p*(*n*) a-SiC/*n*(*p*) c-Si heterojunction solar cells with different thicknesses of the a-SiC:H layer. The dashed line represents the experimental *I-V* curve for the *p* a-SiC/*n* c-Si solar cell [3].

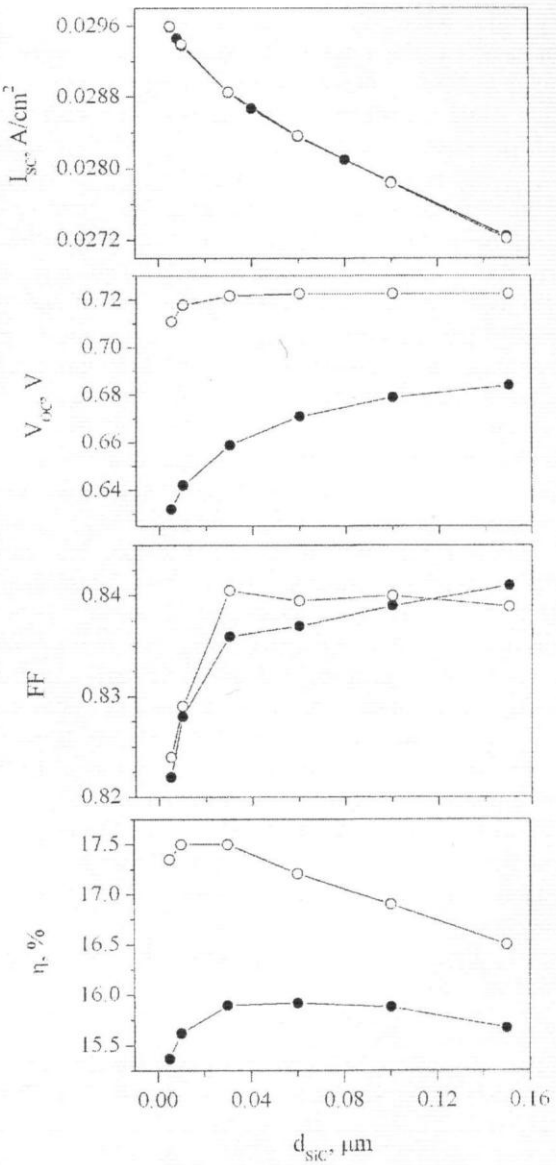

Fig. 3. Photovoltaic parameters: short circuit current (I_{SC}), open circuit voltage (V_{OC}), filling factor (FF) and cell efficiency (η) for the *p-n* (full circle) and *n-p* (open circle) heterojunctions.

The photovoltaic characteristics I_{SC}, V_{OC}, FF, and η of the hybrid tandems are presented in Fig. 3. The short circuit current is found to decrease with increasing d_{SiC} for both types of heterojunctions. For the open circuit voltage, different behaviors of this parameter are observed in the *p-n* and *n-p* heterostructures. In the case of the *p-n* junction, V_{OC} gradually increases with d_{SiC}, whereas for the *n-p* structure this parameter is small sensitive to the thickness of the amorphous layer. The open circuit voltage is lower in the *p-n* structure compared to that in the *n-p* tandem by approximately 0.04 V. The filling factor sharply rises on approaching $d_{SiC} = 0.03$ μm, and above this thickness it changes insignificantly. Finally, we note that the cell efficiency η of the *n-p* heterostructure is higher than that of the *p-n*

one, which is mainly due to high values of open circuit voltages V_{OC} in the first heterojunction. Besides, η reaches a maximum value for the *n-p* and *p-n* heterostructures having the amorphous layer thicknesses, d_{SiC} = 0.03 μm and 0.03-0.06 μm, respectively. These values are very close to those established for the experimental *p-n* structures (d_{SiC} ~ 0.03-0.04 μm for the *p-n* heterojunctions) [3-4]. In the first approximation, one can say that the correlation between η and V_{OC} takes place. However, at large values of amorphous layer thicknesses, lowering I_{SC} with increasing d_{SiC} leads to the decreasing cell efficiency, despite an insignificant increase in the open circuit voltage. Large thicknesses of the a-SiC:H layer prevent a collection of photogenerated carriers near the amorphous/crystalline interface. As a result, the gradually reduction of the short circuit current with increasing d_{SiC} takes place.

In order to explain the fact that the values V_{OC} are higher in the *n-p* cell as compared to those in the *p-n* structure, we have calculated the open circuit voltage as a function of the valence band tail width, T_V. The results of such calculations are shown in Fig. 4. At the same doping level, the open circuit voltage is higher in the *p-n* heterostructures with the smallest T_V. The smaller is T_V, the higher V_{OC} is. This occurs owing to narrowing the mobility gap because of an increase in the valance band edge mobility E_V (cf. Fig. 4). The similar results were obtained for the $V_{OC}(T_C)$ dependence (not shown). In all heterostructures under consideration, we accept $T_V > T_C$, in agreement with the tight binding band structure of a-SiC:H [5] and with the simulation models involving amorphous silicon or silicon carbide layers [1-3, 6, 8]. In the *n-p* structure, the donor states are located inside the conduction band tail that is narrower compared to the valence band tail (Table). It follows that the mobility gap in the *n-p* tandem will be larger than in the *p-n* one.

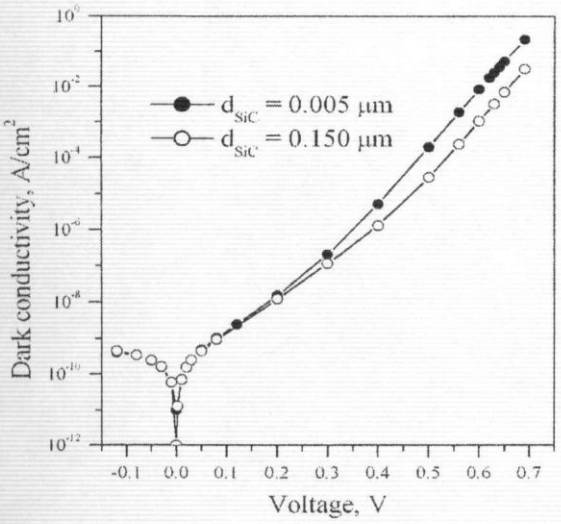

Fig. 4. Dependences of the open circuit voltage (V_{OC}) and the energetic distance between the Fermi energy (E_F) and the valance band edge mobility (E_V) on the width of the valence band tail (T_V) in the *p* a-SiC/*n* c-Si heterojunction.

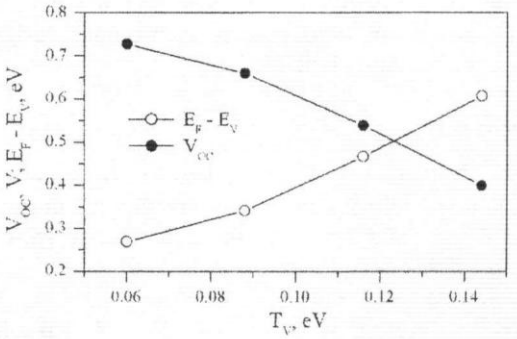

Fig. 5. Dark *I-V* characteristics of the *p* a-SiC:H/*n* c-Si device with different amorphous layer thicknesses, d_{SiC}.

Given this finding, one can suppose that V_{OC} in the *n-p* tandems will be higher than in the *p-n* structures, in agreement with the simulated results (cf. Fig. 3). As a result, the cell efficiency of the *n-p* heterostructures will be higher as compared to that of the *p-n* heterojunctions.

To investigate the effect of the amorphous layer thickness on the dark characteristics, we have calculated the dark *I-V* dependences for the *p-n* heterojunctions with various values of d_{SiC}. These characteristics are shown in Fig. 5. It is seen that at small voltages the dark *I-V* dependences of the *p* a-SiC:H/*n* c-Si devices are small sensitive to d_{SiC}. At high voltages, the current is higher in the structure with d_{SiC} = 0.005 μm than in the structure with d_{SiC} = 0.15 μm. Thus, the light and dark photovoltaic characteristics point to dropping current with increasing the thickness of the a-SiC:H layer in the hybrid heterostructures.

4. Conclusion

We have developed a scheme for simulations of photovoltaic properties of hybrid solar cells based on a-SiC:H/c-Si heterojunctions. Both the *p-n* and *n-p* heterojunction solar cells were investigated. The simulation results reveal the sensitivity of the photovoltaic parameters to the thickness of the a-SiC:H layer. The increase in the thickness of the a-SiC:H layer, d_{SiC}, prevents a collection of photogenerated carriers near the amorphous/crystalline interface. As a result, the gradually reduction of the short circuit current with increasing d_{SiC} takes place. On the contrary, the open circuit voltage increases with d_{SiC} in both the heterojunctions, and for the *n-p* tandem reaches saturation at d_{SiC} > 0.03 μm. The correlation between the filling factor and open circuit voltage is observed. The cell efficiency reaches a maximum value for d_{SiC} = 0.03 μm and 0.03-0.06 μm for the *n-p* and *p-n* heterostructures, respectively. The open circuit voltage and, correspondingly, cell efficiency of the *n-p* heterostructures are higher compared to those of the *p-n* heterojunctions. The dark *I-V* characteristics of the *p* a-SiC:H/*n* c-Si devices point to increasing the current with

reducing d_{SiC}. Finally, we suppose that the developed scheme can be used to predict the optimal design of other similar photovoltaic devices.

References

1. Y. Hamakawa, A technological evolution from bulk crystalline age to multilayers thin film age in solar photovoltaics // *Renewable Energy* **15**, p. 22-31 (1998).
2. M.W.M. van Cleef, F.A. Rubinelli, J.K. Rath, R.E.I. Scropp, W.F. van der Weg, R. Rizzoli, C. Summonte, R. Pinghini, E. Centurioni and R. Galloni, Photocarrier collection in a-SiC:H/c-Si heterojunction solar cells // *J. Non-cryst. Solids* **227-230**, p. 1291-1294 (1998).
3. M.W.M. van Cleef, F.A. Rubinelli, R. Rizzoli, R. Pinghini, R.E.I. Schropp and W.F. van der Weg, Amorphous silicon carbide/crystalline Silicon heterojunction solar cells: a comprehensive study of the photocarrier collection // *Jpn. J. Appl. Phys.* **37**, p. 3926-3932 (1998).
4. J. Pallares and R.E.I. Schropp, Role of the buffer layer in the active junction in amorphous-crystalline silicon heterojunction solar cells // *J. Appl. Phys.* **88**, p. 293-299 (2000).
5. V.I. Ivashchenko, P.E.A. Turchi, V.I. Shevchenko, L.A. Ivashchenko, and G. V. Rusakov, Atomic and electronic structures of a-SiC:H from tight binding-molecular dynamics // *J. Phys: Condens. Matter*, **15**, p. 4119-4126 (2003).
6. V. Cech, Modeling of the I-V characteristics in amorphous silicon n^+-i-n^+ devices // *J. Appl. Phys.* **88**, p. 5374-5380 (2000).
7. I. Chan and S. Lee, On the current-voltage characteristics of amorphous hydrogenated silicon diodes // *J. Appl. Phys.* **53,** p. 1045-105 (1982).
8. P. Sichanugris, M. Konagi and K. Takahashi, Theoretical analysis of amorphous silicon solar cells: Effects of interface recombination // *J. Appl. Phys.* **55**, p. 1155-1161 (1984).
9. P. Cova, A. Singh and R.A. Masut, Simultaneous analysis of current-voltage and capacitance-voltage characteristics of metal-insulator-semiconductor diodes with a high mid-gap trap density // *J. Appl. Phys.* **85**, p. 6530-6538 (1999).
10. H.Z. Fardi, D.W. Winston, R.E. Uayes, M.C. Hanna // *IEEE Trans. Electron Devices* **47**, p. 915-919 (2000).